ACS Macro Letters

Letter

pubs.acs.org/macroletters

Influence of Composition Fluctuations on the Linear Viscoelastic Properties of Symmetric Diblock Copolymers near the Order–Disorder Transition

Robert J. Hickey,[†,§] Timothy M. Gillard,[‡,§] Timothy P. Lodge,*[,†,‡] and Frank S. Bates*[,‡]

[†]Department of Chemistry and [‡]Department of Chemical Engineering and Materials Science, University of Minnesota, Minneapolis, Minnesota 55455, United States

Supporting Information

ABSTRACT: Rheological evidence of composition fluctuations in disordered diblock copolymers near the order–disorder transition (ODT) has been documented in the literature over the past three decades, characterized by a failure of time–temperature superposition (tTS) to reduce linear dynamic mechanical spectroscopy (DMS) data in the terminal viscoelastic regime to a temperature-independent form. However, for some materials, most notably poly(styrene-*b*-isoprene) (PS–PI), no signature of these rheological features has been found. We present small-angle X-ray scattering (SAXS) results on symmetric poly(cyclohexylethylene-*b*-ethylene) (PCHE–PE) diblock copolymers that confirm the presence of fluctuations in the disordered state and DMS measurements that also show no sign of the features ascribed to composition fluctuations. Assessment of DMS results published on five different diblock copolymer systems leads us to conclude that the effects of composition fluctuations can be masked by highly asymmetric block dynamics, thereby resolving a long-standing disagreement in the literature and reinforcing the importance of mechanical contrast in understanding the dynamics of ordered and disordered block polymers.

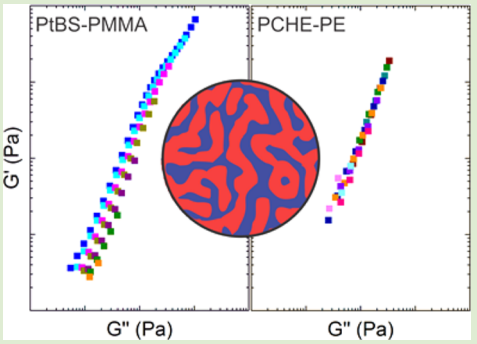

Materials with nanoscale features are being incorporated into emerging technologies with applications in energy,[1] electronics,[2] and medicine.[3] Block polymers are a class of materials for which synthetic methods offer precise control over chemical architecture, morphology, dynamics, and morphological length scale.[4] As a consequence, they are an active area of research with potential uses in a diverse array of products, including batteries,[5] lithographic materials,[6] and drug delivery.[7] A fundamental understanding of block polymer phase transitions, nanoscale morphologies, and processing is an essential prerequisite to integration into future commercial products.[8,9] It is well established that volumetrically symmetric AB diblock copolymers (f = 1/2) of finite molecular weight undergo an order–disorder phase transition (ODT) characteristic of the Brazovskii class, for which the change from an ordered lamellar phase (LAM) to an isotropic disordered phase (DIS) is weakly first-order.[10−13] Thermally driven fluctuations in local composition profoundly influence block copolymer phase behavior near this fluctuation-induced phase transition, destroying the second-order ODT anticipated by mean-field theory (i.e., infinite molecular weight limit).[10,14] Here, we present dynamic mechanical spectroscopy (DMS) results that help elucidate how differences in the individual A- and B-block relaxation times of an AB diblock copolymer are manifested in linear oscillatory viscoelastic measurements.

A host of experimental techniques, including small-angle X-ray scattering (SAXS),[15−18] small-angle neutron scattering (SANS),[11,12,19] differential scanning calorimetry (DSC),[13] transmission electron microscopy (TEM),[20−22] rheology,[23−25] and others,[26−32] have confirmed the presence of composition fluctuations in the disordered phase of block polymers near the ODT. Schematic illustrations of the morphology around the LAM–DIS transition for a symmetric diblock copolymer are presented in Figure 1. Below the order–disorder transition temperature (T_{ODT}), a static microphase-separated state with coherent, long-range lamellar order is obtained. In the absence of an aligning field (e.g., hydrodynamic,[33] electric,[34] magnetic[35]), a polycrystalline structure with many randomly arranged LAM grains occurs, where the material is isotropic on long length scales (Figure 1a). Above T_{ODT}, composition fluctuations produce a structured but globally isotropic disordered state characterized by transient microphase separation at the local level, i.e., with short-range correlations but no long-range order (Figure 1b). This fluctuating equilibrium disordered state resembles both a bicontinuous microemulsion and the nonequilibrium structure observed during spinodal decomposition of a binary blend of immiscible liquids.[13,36] While there are obvious differences in the microstructure of the LAM and DIS phases on large length scales (i.e., greater than the periodicity d, where the interfacial curvature is characterized by zero and negative Gauss curvature, respectively), locally (i.e., on the molecular scale) they are quite

Received: January 7, 2015
Accepted: January 29, 2015
Published: February 3, 2015

DOI: 10.1021/acsmacrolett.5b00014
ACS Macro Lett. 2015, 4, 260–265

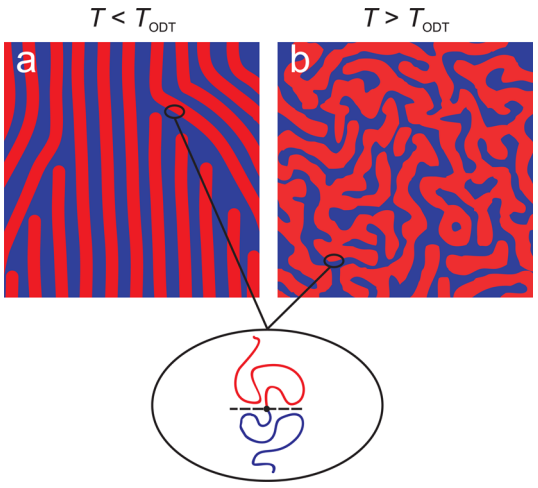

Figure 1. Morphology of the (a) ordered ($T < T_{ODT}$) and (b) fluctuating disordered ($T > T_{ODT}$) states of a diblock copolymer melt.

similar: both contain an AB interface with zero mean curvature separating A- and B-rich domains. Indeed, the local composition profile normal to the AB interface has been shown to be nearly identical in the LAM and DIS phases at the ODT and of relatively high amplitude for experimental molecular weights.[13,37]

Although the first reported experimental evidence of composition fluctuations in block polymers was a rheological feature in the disordered state near the ODT,[23] a comprehensive understanding of the influence of fluctuations on rheology has remained elusive. The rheological feature attributed to composition fluctuations, which we refer to as the "rheological fingerprint", manifests as additional elasticity in the low-frequency ($\omega \ll \tau^{-1}$, where τ is the single chain relaxation time) linear dynamic elastic (G') modulus near the ODT. The associated temperature-dependent onset of terminal relaxation ($G' \sim \omega^2$; $G'' \sim \omega^1$) is clearly evident in master plots prepared using the time−temperature superposition (tTS) principle (i.e., a lack of superposition of G' at low frequencies as the ODT is approached)[38] in certain systems; see Rosedale et al.[25] and Kennemur et al.[24] for clear examples obtained with symmetric poly(ethylene-*alt*-propylene-*b*-ethylethylene) (PEP−PEE) and poly(*t*-butylstyrene-*b*-methyl methacrylate) (PtBS-PMMA) diblock copolymer melts, respectively. In apparent disagreement with these reports, the rheological fingerprint of fluctuations is absent in publications dealing with several other diblock copolymer systems,[39,40] most notably poly(styrene-*b*-isoprene) (PS−PI), leading to skepticism regarding the fluctuation-based interpretation of this dynamical feature.[39] One hypothesis for explaining this relaxation mode implicates polymer chain entanglements.[29,38] However, a recent report dealing with the rheology of unentangled PtBS−PMMA, a system governed by essentially a single glass transition temperature ($T_g \approx 130$ °C), unambiguously shows the rheological fingerprint of composition fluctuations,[24] dispelling this notion.

Here, we present results that connect the rheological fingerprint of composition fluctuations to the ratio of the individual A- and B-block relaxation times of an AB diblock copolymer, a parameter previously referred to as "mechanical contrast".[38] We investigated the rheological response near the ODT of a symmetric poly(cyclohexylethylene-*b*-ethylene) (PCHE−PE) diblock copolymer and compare the data to previously published results, including a reanalysis of the data from the PtBS−PMMA polymer.[24] These samples are referred to as PCHE−PE-14 and PtBS−PMMA-236; synthesis and characterization of these materials is detailed in previously published works.[41,42] These two polymers were chosen because they have similar molecular weights (M_n), 13.6 and 17.6 kg/mol, T_{ODT} values, 189 ± 1 and 193 ± 1 °C, and block volume fractions, $f_{PCHE} = 0.52$ and $f_{PtBS} = 0.53$, respectively. We find that when the single-chain relaxation times (τ) for the individual blocks differ by orders of magnitude (ratio > 10^4) the rheological fingerprint indicative of fluctuations is not found in $G'(\omega)$. This work resolves a long-unanswered question pertaining to the ability to measure rheologically the effects of composition fluctuations and aids in understanding low-frequency scaling for both the dynamic elastic and loss moduli in block copolymers in general.

The presence of fluctuations in disordered PCHE−PE-14 near the ODT ($T > T_{ODT} = 189 \pm 1$ °C) was conclusively established using SAXS experiments. Below T_{ODT}, this material forms an ordered LAM phase with a domain spacing $d = 2\pi/q^* = 17$ nm, where q^* is the scattering wave vector associated with the first-order Bragg reflection ($q = 4\pi\lambda^{-1}\sin(\theta/2)$; λ is the X-ray wavelength; and θ is the scattering angle) (see Supporting Information). In Figure 2, the inverse primary peak intensity, $I^{-1}(q^*)$, is plotted as a function of inverse temperature, T^{-1}. When the sample is heated through the ODT, there is a discontinuous increase in $I^{-1}(q^*)$ and broadening of the primary scattering peak (see Supporting Information), which signifies the transition from an ordered to a disordered state. The concave upward curvature of $I^{-1}(q^*)$ with T^{-1}, which persists to at least 50 °C above T_{ODT}, is indicative of the presence of composition fluctuations in the disordered phase.[11]

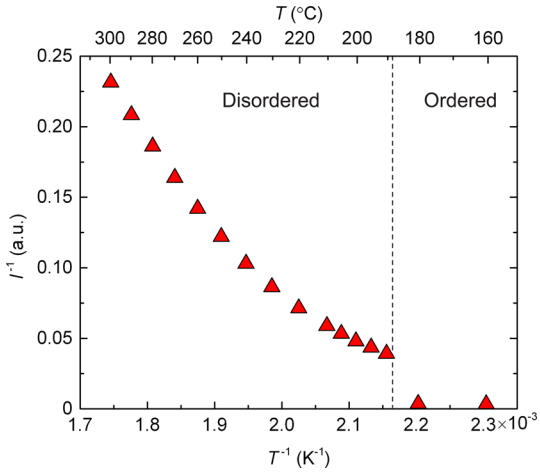

Figure 2. Inverse primary peak intensity, $I^{-1}(q^*)$, versus inverse temperature, T^{-1}, obtained by SAXS while heating sample PCHE−PE-14 from the ordered lamellar phase to temperatures above the order−disorder transition at 189 ± 1 °C (dashed line). Curvature in $I^{-1}(q^*)$ in the disordered state results from composition fluctuations.

The linear dynamic elastic (G') and loss (G'') moduli were measured for PCHE−PE-14 (and PCHE−PE-19; $M_n = 18.9$ kg/mol and $f_{PCHE} = 0.51$; $T_{ODT} = 317$ °C)[41] using a Rheometrics Scientific ARES strain-controlled rheometer with a 25 mm diameter parallel plate geometry over the frequency range $0.01 \le \omega \le 100$ rad/s and $140 \le T \le 260$ °C. Time−temperature shift factors (a_T) were obtained by constructing a master plot for PCHE−PE-19 and application of the Williams−Landel−Ferry (WLF) equation, $\log(a_T) = -c_1(T - T_{ref})/(c_2 +$

DOI: 10.1021/acsmacrolett.5b00014
ACS Macro Lett. 2015, 4, 260−265

$T - T_{ref}$); c_1 = 5.16 and c_2 = 104.25 °C, based on the reference temperature T_{ref} = 180 °C (see Supporting Information). These shift factors were used to construct a master plot for PCHE−PE-14, without any adjustable parameters, as shown in Figure 3.

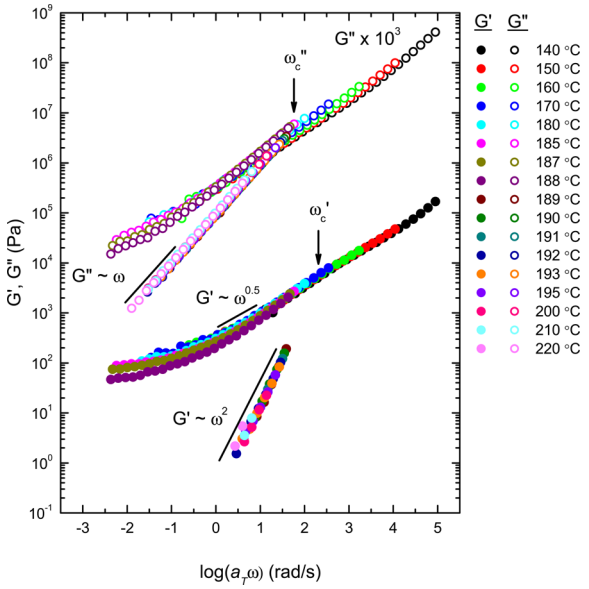

Figure 3. Master plot for the linear dynamic elastic (G') and loss (G'') moduli for PCHE−PE-14 near the order−disorder transition (T_{ODT} = 189 ± 1 °C). Time−temperature shift factors (a_T) were obtained from ordered (lamellae) sample PCHE−PE-19 and applied to PCHE−PE-14 using the reference temperature T_{ref} = 180 °C. The G'' data have been shifted vertically by the factor 10^3 for clarity.

Two distinct branches are evident in $G'(\omega)$ and $G''(\omega)$ for $\omega < \omega_c$, where ω_c marks the point of transition from single chain ($\omega > \omega_c$) to collective (domain) dominated ($\omega < \omega_c$) dynamics.[38] For $T > T_{ODT}$ all the data collapse onto common, temperature-independent, terminal response curves, $G' \sim \omega^2$ and $G'' \sim \omega^1$, while for $T < T_{ODT}$ nonterminal behavior ($G' \sim G'' \sim \omega^\delta$ with $\delta < 1$)[38] is obvious. Significantly, there is no evidence of the composition fluctuations (documented by SAXS, Figure 2) in these results. This result duplicates previous work with another hydrogenated polyolefin diblock copolymer, poly(cyclohexylethylene-*b*-ethylene propylene) (PCHE−PEP), which showed similar tTS master plots in which the rheological fingerprint of fluctuations was not observed.[40]

Although often applied with success to block polymers, the assumptions underlying tTS do not strictly apply to thermorheologically complex systems that have more than one fundamental time constant, e.g., diblock copolymers with two distinct glass transition temperatures (T_g).[38,39] Therefore, plots of log G' vs log G'' (a type of Cole−Cole or Nyquist diagram also referred to by some authors as a Han plot[43]) have been used to display block polymer dynamics and determine T_{ODT} in block copolymer systems; this procedure eliminates the need to apply arbitrary shift factors.[38,43] In Figure 4 the data from Figure 2 (PCHE−PE-14) and the results reported by Kennemur et al.[24] for PtBS−PMMA-236 are replotted in the Cole−Cole format. There are striking similarities between the tTS master plots and the Cole−Cole plots for PCHE−PE and PtBS−PMMA-236.[24] In both depictions, the low modulus regime ($\omega < \omega_c$) shows two branches corresponding to the disordered ($T > T_{ODT}$) and ordered ($T < T_{ODT}$) phases. The disordered state branch in the Cole−Cole construction for both

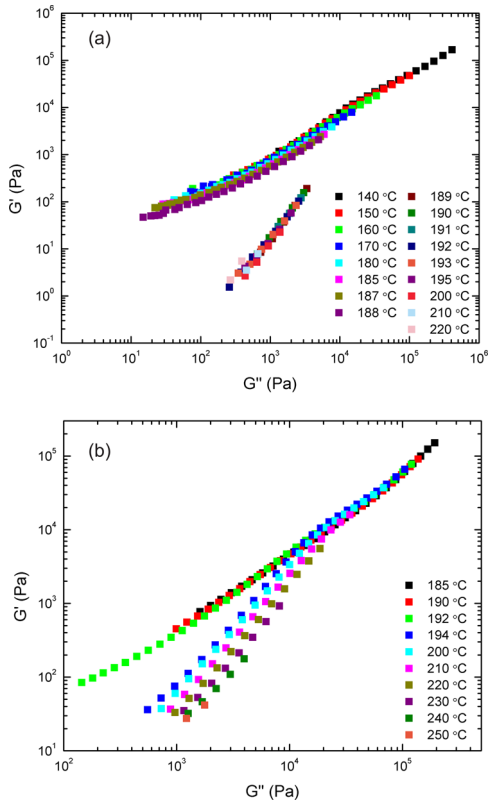

Figure 4. Modified Cole−Cole plots for (a) PCHE−PE-14 and (b) PtBS−PMMA-236. The order−disorder transition for these materials occurs at 189 ± 1 °C and 193 ± 1 °C, respectively. The temperature dependence of the low-frequency response in G' in panel (b) is attributed to composition fluctuations. Absence of this feature in (a) is associated with highly asymmetric block relaxation times.

polymers shows behavior analogous to the low-frequency branches in the tTS master plots. Specifically, near perfect overlay of the data is obtained for all temperatures in PCHE−PE-14, while the rheological fingerprint of fluctuations is plainly evident in both the tTS and Cole−Cole constructions for PtBS−PMMA-236. These comparisons validate the use of the tTS procedure for both specimens.

These results raise an intriguing question: Why do PCHE−PE-14 and PtBS−PMMA-236, which exhibit comparable fluctuating disordered states (as confirmed by SAXS) and have similar physical properties (M_n and T_{ODT}), exhibit qualitatively different viscoelastic responses just above the T_{ODT}? We propose that this difference can be traced to the relative relaxation times for the individual blocks of the diblock copolymers, which is controlled primarily by differences in the glass transition temperatures and to a lesser extent by the relative extents of entanglement. For the PCHE−PE system $T_{g,PCHE}$ = 140 °C, and $T_{g,PE}$ = −120 °C ($\Delta T_g = T_{g,PCHE} - T_{g,PE} \approx 260$ °C). The PCHE block is unentangled ($M_e \cong 40$ kg/mol),[44] while the PE block is entangled ($M_e \cong 0.8$ kg/mol).[44] For PtBS−PMMA neither block is entangled, and $T_{g,PtBS}$ = 141 °C and $T_{g,PMMA}$ = 110 °C system ($\Delta T_g \approx 20$ °C). However, based on DSC measurements near T_{ODT}, PtBS−PMMA-236 exhibits essentially a single glass transition temperature $T_g \approx$ 130 °C.[24]

The ratio of relative block relaxation times, $\tau_r = \tau_A/\tau_B > 1$, for five AB diblock copolymer systems investigated using DMS has been estimated based on the corresponding homopolymer

DOI: 10.1021/acsmacrolett.5b00014
ACS Macro Lett. 2015, 4, 260−265

single-chain longest relaxation times, evaluated at temperatures near the reported T_{ODT} values based on published tTS shift factors.[25,45−50] Rouse ($\tau_1 \sim M_n^2$) or reptation ($\tau_{rep} \sim M_n^{3.4}$) single-chain relaxation times were estimated for the unentangled or entangled homopolymer chains, respectively, using the crossover point, $G'(\omega) = G''(\omega)$, in DMS spectra. As shown in Table 1, the three diblock copolymer systems that exhibit the rheological fingerprint of fluctuations, poly(1,2-butadiene-*b*-1,4-butadiene) (1,2-PBD−1,4-PBD),[23] PEP−PEE,[25] and PtBS−PMMA,[24] have estimated τ_r values near unity,[23−25] which we categorize as relatively low mechanical contrast. Conversely, the diblock copolymer systems that do not exhibit the rheological fingerprint of fluctuations, PS−PI and PCHE−PE, exhibit $\tau_r > 10^4$, which we associate with large mechanical contrast.[39,40] When calculating the 1,2-PBD−1,4-PBD and PEP−PEE single-chain relaxation times, we have used homopolymer T_g values, which likely overestimates the true ΔT_g resulting in a somewhat inflated τ_r (see Supporting Information for an estimate on the magnitude of this effect for 1,2-PBD−1,4-PBD). For example, Kennemur et al.[42] showed using a DSC measurement that $\Delta T_g \cong 0$ for PtBS−PMMA-236 due to mixing of the blocks across the domain interfaces; similar effects occur with the other systems near T_{ODT}.[51,52] Also, we have assumed that the different blocks of the diblock copolymers relax independently and ignore the fact that they are tethered to the interface. While these idealizations are not strictly valid, especially in the case of entangled blocks, we believe the ratio τ_r, based on the estimated values for τ_A and τ_B, provide valuable insight into the influence of chain dynamics on the viscoelastic response in block polymers.

Table 1. Calculated Ratio of Relative Block Relaxation Times, $\tau_r = \tau_A/\tau_B$, for Five AB Diblock Copolymer Systems

diblock copolymer	chain M_w (kg/mol)[a]	$\tau_r = \tau_A/\tau_B$	rheological fingerprint[b]
PCHE−PE T = 190 °C	PCHE (7.6)[45] PE (6.0)[46]	3×10^4	no
PtBS−PMMA T = 180 °C	PtBS (8.4) PMMA (9.3)	≈1[c]	yes[24]
PS−PI T = 180 °C	PS (10.7)[47] PI (10.3)[48]	4×10^4	no[39]
1,2-PBD−1,4-PBD T = 100 °C	1,2 PBD (50.4)[49] 1,4 PBD (30.9)[50]	30[d]	yes[23]
PEP−PEE T = 96 °C	PEP (28.0)[25] PEE (22.0)[25]	4	yes[25]

[a]References indicate where longest relaxation times were determined for the respective homopolymers. [b]References indicate publications where diblock copolymer rheology exhibited the rheological fingerprint. [c]The ratio τ_r was assumed to be approximately 1 since both blocks are unentangled and exhibit an identical T_g. [d]$\tau_r \approx 3$ using measured ΔT_g for the block polymer versus homopolymer T_g's (see Supporting Information).

How the single-chain relaxation time for the individual blocks influences expression of composition fluctuations in the disordered state is not directly obvious. We first consider hypothetical modes of relaxation as the frequency is swept from high ($\omega \gg \omega_c$) to low ($\omega \ll \omega_c$) values in the ordered LAM state. Figure 5 depicts the configurational changes that occur during stress relaxation after an applied step shear strain. In the initial state, prior to any applied strain, the polymer blocks have random walk configurations (subject to the constraints imposed by localizing the junction at the interface). In response to the imposition of an instantaneous step shear strain (parallel to the interface) both blocks deform affinely. For a dynamically symmetric system the blocks will relax simultaneously leading to recovery of the initial random walk configuration. However, a dynamically asymmetric system, e.g., $\tau_r \gg 1$, will behave quite differently. Using PCHE−PE as the example, after time $\tau_{PE} \ll t \ll \tau_{PCHE} < \omega_c^{-1}$ the PE block will be fully relaxed, and the stress supported by the material will be essentially entirely borne by the PCHE blocks. (Here we note that the disparity in relaxation times for PCHE−PE, $\tau_r > 10^4$, is dominated by ΔT_g, which overwhelms the effects due to differences in M_e.) At longer times, $\tau_{PE} \ll \tau_{PCHE} < t$, the entire diblock copolymer molecule is relaxed. At long times ($t > \omega_c^{-1}$) $G'(\omega)$ and $G''(\omega)$ reflect interfacial dynamics mediated by interfacial tension and diffusion of diblock copolymers parallel and perpendicular to the interface.[38] The longest-time dynamical modes ($\omega \to 0$) are sensitive to the detailed state of order, including the domain geometry (e.g., lamellae versus cylinders), correlation length, and polycrystalline grain structure.[38]

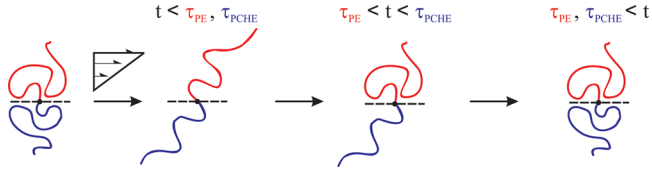

Figure 5. Scheme depicting single-chain stress relaxation for dynamically asymmetric PCHE−PE-14 in the ordered or fluctuating disordered state. The relaxation time (τ) for the PE block (red) is orders of magnitude smaller than for the PCHE block (blue) primarily due to the large disparity in glass transition temperatures (see Table 1).

This picture is helpful when interpreting differences in the low-frequency response of dynamically symmetric and asymmetric block polymers. When $\omega \gg \omega_c$, single-chain dynamics dominate, and $G'(\omega)$ and $G''(\omega)$ are insensitive to the morphology. For $\omega < \omega_c$ the detailed morphology directly influences the viscoelastic behavior.[38] A single lamellar crystal will have a viscoelastic response that depends on its orientation relative to the flow field. When the lamellae are arranged parallel to the shear plane we anticipate Maxwell-like behavior,[53] where the two domains are coupled in series. In the case of dynamically asymmetric block polymers, the mechanical response is dominated by the dynamically faster blocks. In the perpendicular orientation (shear direction parallel to the lamellar normal) parallel coupling of the domains will produce a Voigt-like mechanical response that is instead dominated by the slower relaxing blocks for dynamically asymmetric block polymers.[53] A polycrystalline morphology averages these effects over all orientations, which produces the documented $G' \sim G'' \sim \omega^{1/2}$ scaling observed experimentally for $\omega \ll \omega_c$ for both dynamically symmetric and asymmetric block polymers (although at the lowest frequencies ($\omega \to 0$) a polycrystalline lamellar morphology may exhibit solid-like behavior ($G' \sim \omega^0$) due to the presence of grain boundaries).[38] Several theories have been developed to describe this low-frequency power law behavior,[38,54,55] for example based on mode coupling,[54] entanglement,[55] and excess chain density equilibration concepts.[55]

DOI: 10.1021/acsmacrolett.5b00014
ACS Macro Lett. 2015, 4, 260−265

At the lowest frequencies ($\omega \ll \omega_c$) the fluctuating disordered phase is a fluid exhibiting terminal scaling ($G' \sim \omega^2$ and $G'' \sim \omega^1$) implying that the bicontinuous composition pattern (Figure 1, $T > T_{ODT}$) can be reorganized to remain isotropic in response to an applied strain. Apparently, mechanical contrast plays a significant role in setting the temperature-dependent time constant for relaxing composition fluctuations. We believe this result can be explained using the concepts associated with the orientation dependence of stress relaxation in ordered lamellae. As the ODT is approached in the disordered state the spatial range of correlations between locally segregated domains increases; i.e., at a local level the morphology is increasingly lamellar-like. Due to the isotropic nature of the fluctuating regions and the absence of fixed boundaries (i.e., grain boundaries as in the polycrystalline state) there will always be regions with a parallel orientation within a few periods of a correlated set of fluctuating domains with perpendicular alignment. Stress relaxation will be controlled by slip in these parallel regions as the ODT is approached. In systems with large mechanical contrast slip occurs in the dynamically fast domains, masking the consequences of the structural heterogeneities, analogous to the linear viscoelastic response of a suspension of solid particles dispersed in a simple fluid. In the absence of mechanical contrast the restrictions to molecular motion imposed by localization of the block copolymer chains at the domain interfaces lead to an additional mode of relaxation, which emerges at $\omega \leq \omega_c$.

Over the past 30 years, contradictory dynamic mechanical spectroscopy results concerning composition fluctuations in diblock copolymer systems have led to questions regarding the validity of experimentally probing the character of the ODT with rheology. This work demonstrates that highly asymmetric block dynamics, i.e., characterized by large mechanical contrast, eliminates the rheological fingerprint of fluctuations found in dynamically symmetric diblock copolymers. This finding has the potential to impact the theory of stress-relaxation mechanisms for ordered and disordered phases and shear-induced alignment of block polymers.[9,33,38,56−59]

■ ASSOCIATED CONTENT

Supporting Information

Detailed DMS and SAXS experimental procedures. This material is available free of charge via the Internet at http://pubs.acs.org.

■ AUTHOR INFORMATION

Corresponding Authors

*E-mail: bates001@umn.edu

*E-mail: lodge@umn.edu.

Author Contributions

§These authors contributed equally.

Notes

The authors declare no competing financial interest.

■ ACKNOWLEDGMENTS

We thank Justin Kennemur for providing the PtBS-PMMA raw rheology data and David Morse for useful discussion. This research was supported by the National Science Foundation under Award DMR-1104368. Portions of this work were performed at the DuPont−Northwestern−Dow Collaborative Access Team (DND-CAT) located at Sector 5 of the Advanced Photon Source (APS). DND-CAT is supported by E.I. DuPont de Nemours & Co., The Dow Chemical Company, and Northwestern University. Use of the APS, an Office of Science User Facility operated for the U.S. Department of Energy (DOE) Office of Science by Argonne National Laboratory, was supported by the U.S. DOE under Contract No. DE-AC02-06CH11357.

■ REFERENCES

(1) Orilall, M. C.; Wiesner, U. *Chem. Soc. Rev.* **2011**, *40*, 520−535.

(2) Sanchez, C.; Belleville, P.; Popall, M.; Nicole, L. *Chem. Soc. Rev.* **2011**, *40*, 696−753.

(3) Shi, J.; Votruba, A. R.; Farokhzad, O. C.; Langer, R. *Nano Lett.* **2010**, *10*, 3223−3230.

(4) Bates, F. S.; Hillmyer, M. A.; Lodge, T. P.; Bates, C. M.; Delaney, K. T.; Fredrickson, G. H. *Science* **2012**, *336*, 434−440.

(5) Hallinan, D. T.; Balsara, N. P. *Annu. Rev. Mater. Res.* **2013**, *43*, 503−525.

(6) Bates, C. M.; Maher, M. J.; Janes, D. W.; Ellison, C. J.; Willson, C. G. *Macromolecules* **2013**, *47*, 2−12.

(7) Duncan, R. *Nat. Rev. Drug Discovery* **2003**, *2*, 347−360.

(8) Lodge, T. P. *Macromol. Chem. Phys.* **2003**, *204*, 265−273.

(9) Chen, Z.-R.; Kornfield, J. A.; Smith, S. D.; Grothaus, J. T.; Satkowski, M. M. *Science* **1997**, *277*, 1248−1253.

(10) Fredrickson, G. H.; Helfand, E. *J. Chem. Phys.* **1987**, *87*, 697−705.

(11) Bates, F.; Rosedale, J.; Fredrickson, G.; Glinka, C. *Phys. Rev. Lett.* **1988**, *61*, 2229−2232.

(12) Bates, F. S.; Rosedale, J. H.; Fredrickson, G. H. *J. Chem. Phys.* **1990**, *92*, 6255−6270.

(13) Lee, S.; Gillard, T. M.; Bates, F. S. *AIChE J.* **2013**, *59*, 3502−3513.

(14) Leibler, L. *Macromolecules* **1980**, *13*, 1602−1617.

(15) Hashimoto, T.; Shibayama, M.; Kawai, H. *Macromolecules* **1983**, *16*, 1093−1101.

(16) Roe, R.-J.; Fishkis, M.; Chang, J. C. *Macromolecules* **1981**, *14*, 1091−1103.

(17) Sakamoto, N.; Hashimoto, T. *Macromolecules* **1995**, *28*, 6825−6834.

(18) Zhao, Y.; Sivaniah, E.; Hashimoto, T. *Macromolecules* **2008**, *41*, 9948−9951.

(19) Rosedale, J. H.; Bates, F. S.; Almdal, K.; Mortensen, K.; Wignall, G. D. *Macromolecules* **1995**, *28*, 1429−1443.

(20) Hashimoto, T.; Sakamoto, N. *Macromolecules* **1995**, *28*, 4779−4781.

(21) Hashimoto, T.; Sakamoto, N.; Koga, T. *Phys. Rev. E* **1996**, *54*, 5832−5835.

(22) Sakamoto, N.; Hashimoto, T. *Macromolecules* **1998**, *31*, 3815−3823.

(23) Bates, F. S. *Macromolecules* **1984**, *17*, 2607−2613.

(24) Kennemur, J. G.; Hillmyer, M. A.; Bates, F. S. *ACS Macro Lett.* **2013**, *2*, 496−500.

(25) Rosedale, J. H.; Bates, F. S. *Macromolecules* **1990**, *23*, 2329−2338.

(26) Dalvi, M.; Eastman, C.; Lodge, T. *Phys. Rev. Lett.* **1993**, *71*, 2591−2594.

(27) Dalvi, M. C.; Lodge, T. P. *Macromolecules* **1994**, *27*, 3487−3492.

(28) Jian, T.; Anastasiadis, S. H.; Semenov, A. N.; Fytas, G.; Adachi, K.; Kotaka, T. *Macromolecules* **1994**, *27*, 4762−4773.

(29) Jin, X.; Lodge, T. *Rheol. Acta* **1997**, *36*, 229−238.

(30) Kannan, R. M.; Su, J.; Lodge, T. P. *J. Chem. Phys.* **1998**, *108*, 4634−4639.

(31) Stepanek, P.; Lodge, T. P. *Macromolecules* **1996**, *29*, 1244−1251.

(32) Stuehn, B.; Stickel, F. *Macromolecules* **1992**, *25*, 5306−5312.

(33) Chen, Z.-R.; Kornfield, J. A. *Polymer* **1998**, *39*, 4679−4699.

(34) Xu, T.; Zhu, Y.; Gido, S. P.; Russell, T. P. *Macromolecules* **2004**, *37*, 2625−2629.

(35) Tran, H.; Gopinadhan, M.; Majewski, P. W.; Shade, R.; Steffes, V.; Osuji, C. O.; Campos, L. M. *ACS Nano* **2013**, *7*, 5514−5521.

DOI: 10.1021/acsmacrolett.5b00014
ACS Macro Lett. 2015, 4, 260−265

(36) Jones, B. H.; Lodge, T. P. *Polym. J.* **2012**, *44*, 131−146.
(37) Glaser, J.; Medapuram, P.; Beardsley, T. M.; Matsen, M. W.; Morse, D. C. *Phys. Rev. Lett.* **2014**, *113*, 068302.
(38) Fredrickson, G. H.; Bates, F. S. *Annu. Rev. Mater. Sci.* **1996**, *26*, 501−550.
(39) Choi, S.; Han, C. D. *Macromolecules* **2004**, *37*, 215−225.
(40) Gehlsen, M. D.; Bates, F. S. *Macromolecules* **1993**, *26*, 4122−4127.
(41) Habersberger, B. M.; Gillard, T. M.; Hickey, R. J.; Lodge, T. P.; Bates, F. S. *ACS Macro Lett.* **2014**, *3*, 1041−1045.
(42) Kennemur, J. G.; Hillmyer, M. A.; Bates, F. S. *Macromolecules* **2012**, *45*, 7228−7236.
(43) Han, C. D.; Kim, J. *J. Polym. Sci., Part B* **1987**, *25*, 1741−1764.
(44) Fetters, L. J.; Lohse, D. J.; Richter, D.; Witten, T. A.; Zirkel, A. *Macromolecules* **1994**, *27*, 4639−4647.
(45) Zhao, J.; Hahn, S. F.; Hucul, D. A.; Meunier, D. M. *Macromolecules* **2001**, *34*, 1737−1741.
(46) Vega, J. F.; Aguilar, M.; Martínez-Salazar, J. *J. Rheol.* **2003**, *47*, 1505−1521.
(47) Baumgaertel, M.; Schausberger, A.; Winter, H. H. *Rheol. Acta* **1990**, *29*, 400−408.
(48) Abdel-Goad, M.; Pyckhout-Hintzen, W.; Kahle, S.; Allgaier, J.; Richter, D.; Fetters, L. J. *Macromolecules* **2004**, *37*, 8135−8144.
(49) Roovers, J.; Toporowski, P. M. *Macromolecules* **1992**, *25*, 3454−3461.
(50) Baumgaertel, M.; De Rosa, M. E.; Machado, J.; Masse, M.; Winter, H. H. *Rheol. Acta* **1992**, *31*, 75−82.
(51) Bates, F. S.; Bair, H. E.; Hartney, M. A. *Macromolecules* **1984**, *17*, 1987−1993.
(52) Bates, F. S.; Rosedale, J. H.; Bair, H. E.; Russell, T. P. *Macromolecules* **1989**, *22*, 2557−2564.
(53) Hiemenz, P. C.; Lodge, T. P. *Polymer Chemistry*, 2nd ed.; CRC Press: Boca Raton, FL, 2007.
(54) Kawasaki, K.; Onuki, A. *Phys. Rev. A* **1990**, *42*, 3664−3666.
(55) Rubinstein, M.; Obukhov, S. P. *Macromolecules* **1993**, *26*, 1740−1750.
(56) Hermel, T. J.; Wu, L.; Hahn, S. F.; Lodge, T. P.; Bates, F. S. *Macromolecules* **2002**, *35*, 4685−4689.
(57) Vigild, M. E.; Chu, C.; Sugiyama, M.; Chaffin, K. A.; Bates, F. S. *Macromolecules* **2001**, *34*, 951−964.
(58) Koppi, K. A.; Tirrell, M.; Bates, F. S.; Almdal, K.; Colby, R. H. *J. Phys. II* **1992**, *2*, 1941−1959.
(59) Wiesner, U. *Macromol. Chem. Phys.* **1997**, *198*, 3319−3352.

DOI: 10.1021/acsmacrolett.5b00014
ACS Macro Lett. 2015, 4, 260−265